3D-Printed D-Band Lens Antenna with Gratings Matching Layer for Sensing Applications

Marta Arias Campo[1], Wolfgang Wischmann[1], Peter Uhlig[1], Oliver Litschke[1], Simona Bruni[1]
[1] IMST GmbH, Kamp-Lintfort, Germany, arias@imst.de

***Abstract*— Dielectric lens antennas represent a high-performance, cost-effective solution to provide wideband high gain at sub-THz frequencies. However, in particular in sensing applications, multiple reflections in the interface between the lens and air cause false echoes which may lower the dynamic range and accuracy of the system. In this paper, we present a low-cost polypropylene FFF (Fused Filament Fabrication) 3D printed matching layer solution working at 110−170 GHz, implemented on the surface of an elliptical lens. The false echo power level is reduced in more than 20 dB, keeping the wideband gain (>30 dB) over the whole frequency band.**

***Index Terms*— mm-wave, sub-THz, lens antenna, matching layer, dielectric gratings, FFF 3D printing, leaky-wave feed, FMCW radar, wideband communications.**

I. Introduction: Lens Antennas for Sensing Applications

Sub-THz systems are gaining popularity to be used in mass-market applications, such as high-resolution radar [1] or high-speed communications [2], thanks to the availability of large bandwidth. Sub-THz radar systems are some steps ahead and already a reality, finding applications in many industries, such as hot rolling mills for steel strip fabrication [3] or plastic extrusion production processes [4]. Monitoring in-line production by means of radar measurements reduces waste considerably, increasing the production yield. The use of dielectric lens antennas in these systems allows generating high gain with a compact antenna size, and at a lower cost than e.g. horn antennas [5]. However, lens antennas suffer from multiple reflections [6], which in case of radar systems generate false echoes which decrease the measurement accuracy or even prevent the identification of certain targets. For instance, the monitoring of plastic extrusion processes (i.e. pipe wall thickness and diameter measurements) is based on echo detections. The first echo comes when the pulse hits the first pipe interface (air-plastic), the second when it hits the second interface (plastic-air), and then it repeats on the opposite side of the pipe. In this configuration, also secondary reflections are crucial and the false echo can interfere with the signal reflected from the target, affecting the complete measurement. Although low-permittivity lens antennas have been proposed to mitigate this problem, false echoes are still visible in the measured signal [5].

Many matching layer solutions have been presented in the literature. However, not many examples are available at sub-THz frequencies (100−300 GHz). Homogeneous matching layers are usually proposed in silicon lenses [7], [8]. This choice brings an additional production step, raising the prototype price. The high eccentricity in plastic lens with low permittivity and the lack of suitable materials with the required permittivity (ε_r~1.5), encumbers the implementation of this homogeneous approach. Dielectric corrugations have been as well proposed as an alternative, in several geometries, materials and fabrication processes: silicon lens with pyramidal gratings using laser ablation [9], 3D-printed plastic squared holes [10], and at lower frequencies (60 GHz) 3D-printed alumina [11] or Polylactic acid (PLA) [12] in 1D-rectangular shape. 3D-printed solutions are especially attractive, as they render a low-cost solution in a one-step process. However, the materials which are normally proposed present high dielectric loss [10], [12] or are costly [11].

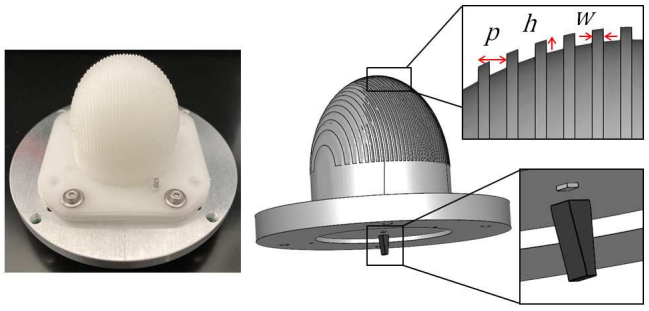

Fig. 1. a) Fabricated lens antenna prototype. b) Lens 3D geometry with a detail of the rectangular gratings on the lens surface and matching pin on the lens bottom side. The leaky-wave cavity is also visible on the bottom, which is fed by a tapered waveguide, described in [13].

In this work, a low cost and easy to produce matching layer solution to minimize false echoes in radar system is presented. The matching structure used is based on dielectric gratings with the geometry presented in [11], using polypropylene material (PP), at D-band frequencies (110−170 GHz). This low-cost plastic is suitable to be used in high-frequency applications, as it presents a very low dielectric loss. Standard FFF 3D printing is used to fabricate the lens and the matching structures. 3D printing fabrication enables producing smaller features with larger aspect ratio than milling processes, especially for soft plastics. The combination of standard 3D printing with the chosen PP material results in a high-performance, low-cost, affordable

solution. The performance of the PP lens with the gratings will be compared with the one reached with the High Density Polyethylene (HDPE) lens presented in [13], from which the waveguide lens feed structure is reused in this work.

II. 3D-Printing Material and Gratings Characterization

The material and corrugations have been characterized as a first step, in order to use the extracted parameters in the final lens design. The first electromagnetic characterization of the material and gratings has been realized at 55–95 GHz, due to the availability of measurement equipment, and in order to prove the usability in different radar frequency bands. Nevertheless, the grating period and width has been maintained equal to the geometry optimized for 140 GHz, and only the grating height has been scaled so that the optimum performance can be measured at 55−95 GHz (Fig. 2a). In this way, the grating production is also validated for D-band.

A. 3D-Printing Material

The dielectric permittivity of the printed material is usually lower than the one of the solid material ($\varepsilon_r = 2.2$ in case of PP), as the relative material volume does not reach 100%, and depends on the process parameters. An accurate evaluation of the material properties, in particular its dielectric permittivity (ε_r), is crucial to calculate the correct lens profile and thus obtain the desired antenna gain. In high-gain lenses, even small errors in the estimation of the material ε_r can lead to large phase errors, lowering significantly their directivity. In order to estimate the ε_r and dielectric loss in the 3D-printed PP material, a slab with 16 mm thickness and 5 cm of diameter has been printed and characterized by means of quasi-optical free-space measurements, using two lens antennas as probes. The estimated parameters for the printed PP are $\varepsilon_r = 2$ and $\tan\delta = 1e-3$.

The low ε_r of PP material is already a good starting point to minimize the reflection in the lens-air surface (−15.3 dB reflection for a flat surface), which leads to a more wideband minimization of the lens internal reflections. Besides, the low ε_r in combination with a leaky-wave feed enables high aperture efficiency over a wide band [13].

B. Gratings Design and Characterization in Planar Slab

The design of the grating has been done taking into account the quantization intrinsic to the FFF 3D-printing process. The chosen grating geometry is 1D-rectangular, as proposed in [11] (Fig. 1b). This structure can be modelled as a homogeneous anisotropic medium [14]. The gratings layer geometry is chosen so that the effective permittivity equals $\sqrt{2}$ for the chosen polarization direction, with a height of $h = \lambda_0/(4\sqrt{2})$, where λ_0 is the wavelength of the center frequency in free space. The designed geometry parameters are shown in Fig. 2a. This geometry has been chosen, as it achieves the highest effective permittivity contrast for a certain minimum dielectric wall thickness. The grating width (400 µm) is chosen to be a multiple of the nozzle diameter (200 µm). This width, in combination with a spacing of 600 µm between gratings, results in the desired effective permittivity for the polarization parallel to the gratings (Fig. 2a). The resulting period for the gratings (1 mm) has been proven to be sufficiently small for the targeted frequency range (110−170 GHz), as shown in Section III.

In order to validate the performance of the 3D-printed gratings, a cylindrical slab with the grating structure printed on one side has been fabricated, with 16 mm thickness and 3 cm diameter (Fig. 2b). As already mentioned, the grating height has been scaled to be characterized at 55−95 GHz ($h = 800\ \mu m$). The gratings geometry has been measured using a 3D laser profilometer. Fig. 2c and d show the results, with a good agreement with the designed gratings height and slightly larger width (420-500 µm). Nevertheless, the low ε_r makes the gratings robust against tolerances, and therefore despite the larger grating width, still a low reflection in the surface (<20 dB) should be reached.

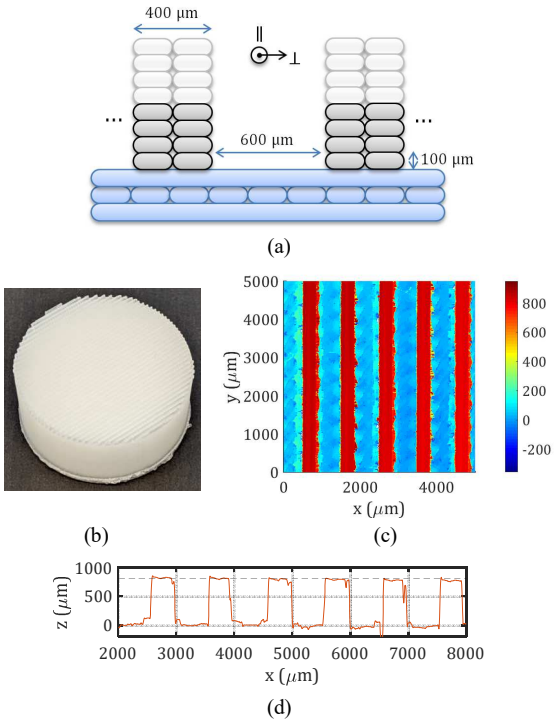

Fig. 2. a) Representation of the FFF 3D-printed gratings geometry for 80 and 140 GHz, showing the printed filaments. Only the number of 3D printed layers changes between the two frequency bands. b) 3D printed PP slab with corrugations at 80 GHz. c) 3D profile measurements of the fabricated gratings. d) 2D profile.

The reflection in the air-gratings surface has been estimated by placing the sample in front of a horn antenna, and measuring the reflected signal coming from the sample

surface. The time-gated results are shown in Fig. 3, where the measurements for the surface with corrugations aligned and orthogonal to the polarization have been compared to the one of the flat PP surface. The reflections have been calibrated with the one of a metallic plate in the same location as the sample surface. Measured results show a more reduced reflection for the polarization orthogonal to the gratings. This can be explained with the wider fabricated gratings (450-500 µm instead of 400 µm) and by considering a higher effective permittivity in the dielectric-filled parts of the gratings (ε_r~2.2) as in the 3D-printed slab (ε_r~2).

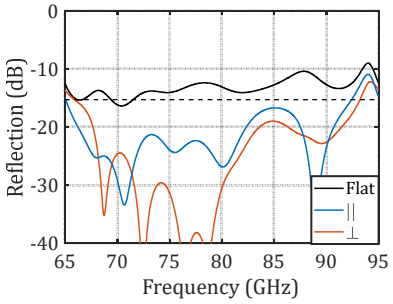

Fig. 3. Time-gated reflection of dielectric grating structure (p =1 mm, h =800 µm, w =400 µm), oriented perpendicularly (⊥) and paralell (∥) to the polarization, compared to a flat 3D-printed surface. The ideal reflection for the flat surface is plotted in dashed line. The reflections are normalized with the one of a metal plate. Measurements performed with horn antenna.

C. Gratings Characterization in Elliptical Lens at W-Band

In order to perform a first validation of the 3D-printing fabrication process of the matching gratings, a lens prototype with gratings has been produced at 80 GHz, with 36 mm diameter. The lens is fed with a waveguide-based leaky-wave feed, which is extensively described in [15], [16]. The false echo reduction has been validated by measuring the reflection in the antenna input when placing a metallic plate in front of the lens at 35.5 cm distance. Results have been compared with a 3D-printed PP lens without corrugations, and a PP lens fabricated with a milling process. Ideally, only the reflection of the plate should be seen in the time-domain results. However, when multiple reflections in the lens are present, a series of false echoes can be seen after the desired reflection. Measurement results in Fig. 4 show approximately 14 dB reduction of the first false echo for the PP with gratings layer with respect to a 3D-printed lens without gratings, and 16 dB when comparing the milled PP lens (smoother surface). Similar false echo reduction is reached when aligning the gratings orthogonally or parallel to the polarization. This result leaves some room for optimization in the fabricated structure, as ideally one of the polarizations should show better performance due to the gratings anisotropic behavior. It should be noted that reflection coming from the metal plate (target) is lower in the milled lens. This is because the same lens geometry has been used as in the 3D printed lenses, even though the milled material is characterized by a higher $\varepsilon_r = 2.2$. This causes phase errors which lead to a lower lens directivity.

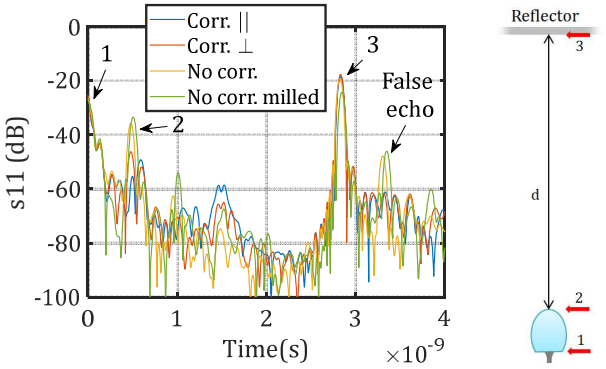

Fig. 4. Measured reflection coefficient of antenna with metal plate at 355 mm distance for the W-band lenses. Hanning window applied to results in frequency domain (65-95 GHz). The arrows point to the reflections in the lens feed, lens-air interface and target, as displayed on the figure on the right. The false echo generated by the lens multiple reflections is also visible.

III. D-Band Lens Antenna Design and Simulations

After validating the reduction of false echoes by means of the fabricated gratings at W-band, the suitability of the FFF 3D-printing process will be demonstrated with a lens design at D-band. An elliptical lens prototype with 35mm diameter has been designed and fabricated at D-band. In this section, simulation results are shown for the 3D-printed PP lens antenna with gratings, and compared with the ones of: 1) a HDPE lens without gratings [13], 2) a PP lens without gratings and 3) a PP lens with a homogeneous matching layer. All lenses are fed with a waveguide-based leaky wave feed with an air cavity, using the split-block described in [13]. Simulations have been performed with the full-wave 3D EM solver EMPIRE XPU [17].

After characterizing the effective permittivity of the 3D-printed PP material, the lens truncation angle has been set to $\theta_e = 44°$, and the lens focus positioned at the feed phase center, which is estimated to be 1.6 mm below the feed ground plane. In order to enhance the feed matching, a squared dielectric pin with 975 µm side and 300 µm height has been placed on the leaky-wave cavity (Fig. 1b). This pin does not affect the feed radiation significantly, preserving the lens directivity. The corrugations in the lens have been built by oversizing the lens in a constant width and creating slots orthogonal to the lens focal plane along the whole surface, as shown in Fig. 1. The gratings height has been set to $h = 420\ \mu m$, considering that 800 µm height showed the best measured performance at ~74 GHz.

The geometry of the fabricated prototype has been mechanically characterized with the laser profilometer (Fig. 5). On the lens top side, results show as well a good agreement in the gratings height, but wider geometry. On the lens side, the gratings height is lower as the designed value (~300 µm). This could be calibrated in later designs.

Nevertheless, the impact of the reflection in this area is lower, thanks to the tapered lens illumination.

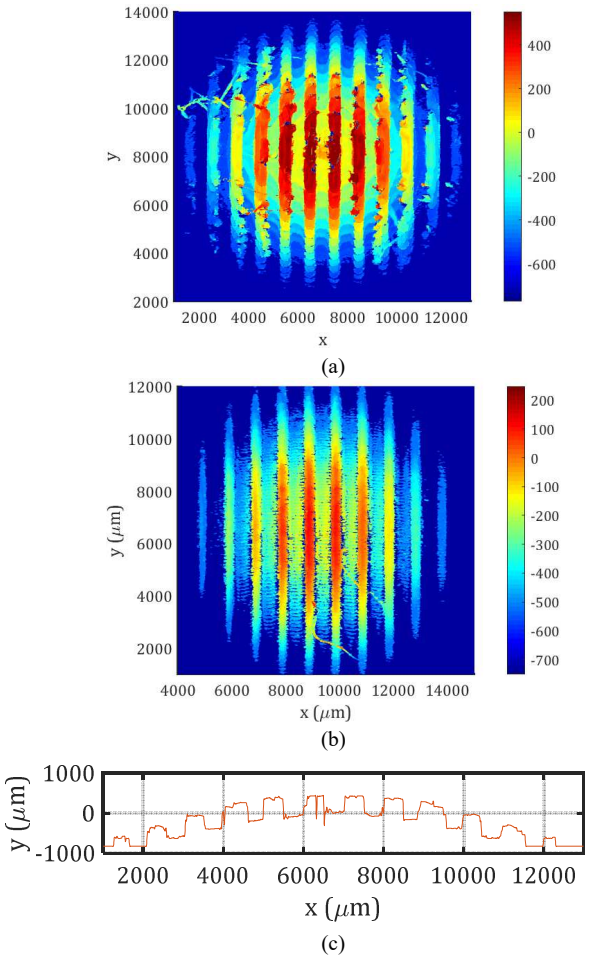

Fig. 5. Profile measurements for the D-band lens prototype (gratings p =1 mm, h =420 µm, w =400 µm). a) 3D profile of lens top side and b) lens side. c) cut along the lens center.

A. Reflection coefficient

The reflection coefficient of the antenna radiating in free space has been simulated and is shown in Fig. 6. Results for the PP with and without corrugations are shown, where the multiple reflection reduction is clearly visible. The matching has been enhanced with respect to the HDPE design in [13], thanks to the lens lower ε_r and by introducing a dielectric pin on the bottom side of the lens, on top of the feeding waveguide (Fig. 1b). Fig. 6a shows as well the time gated reflections of the waveguide-lens interface and the lens-air interface, shown in time domain in Fig. 6b. The reduction of the multiple reflections in the lens-air interface is here as well clear. Fig. 6b shows the time domain reflection coefficient for the PP lens with a $\lambda/4$ homogeneous matching layer (ML), with the same behavior as the solution with gratings.

B. Radiation patterns

The simulated radiation patterns at 140 GHz are shown in Fig. 7a. Results are compared with the lens without corrugations, showing slightly lower side-lobe levels and cross-polar. Fig. 7b shows the antenna directivity over frequency. The lens with corrugations achieves almost the same result as the lens with a homogeneous matching layer (only ~0.2 dB difference in the higher frequencies). The directivity is improved with respect to the antenna without corrugations, thanks to the reduction of reflections loss. The dielectric loss in the lens is lower than 0.4 dB in the whole bandwidth.

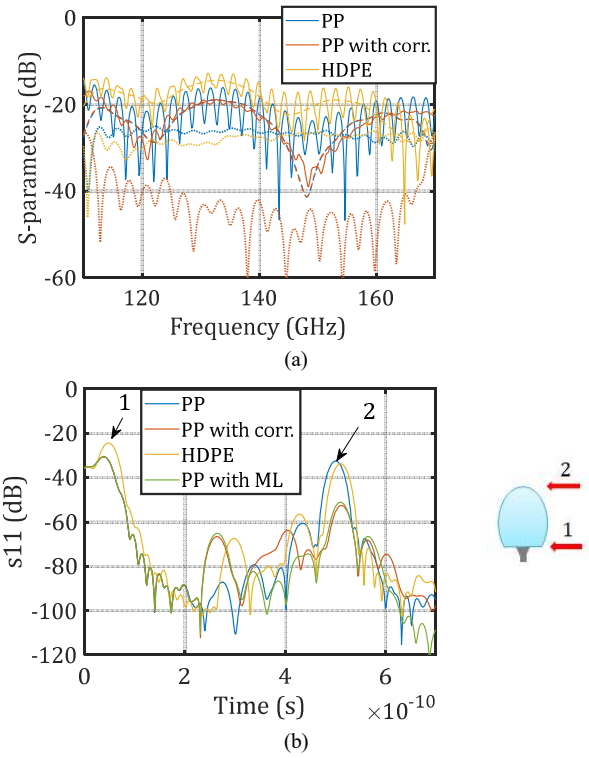

Fig. 6. Reflection coefficient of different lens antennas radiating in free space. a) Frequency domain results. Solid: non-gated, dashed: reflection at waveguide feed time gated (0-0.2ns), dotted: reflection at lens-air interface time gated (0.2-0.65 ns). b) Time domain (Hanning window applied to results in frequency domain). The arrows point to the reflections in the lens feed and lens-air interface, as indicated in the figure on the right.

C. Multiple Reflections Reduction in Radar Measurement

In order to validate the reduction of false echoes in radar measurements thanks to the gratings in the lens, a simulation has been performed with a metallic plate in front of the lens antenna, at 10 cm distance. Results in time domain are shown in Fig. 8. More than 20 dB reduction of the first false echo is reached for the PP with gratings layer, with respect to the HDPE lens in [13]. The reduction is very similar to the one obtained with a homogeneous matching layer.

Measurements for the S-parameters and radiation patterns measurements of the fabricated antenna prototype at D-band are scheduled and will be presented in the conference.

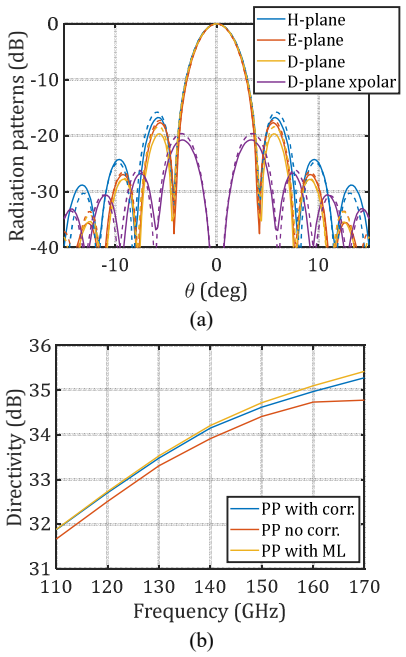

Fig. 7. a) Radiation patterns at 140 GHz. Solid lines: PP lens with corrugations. Dashed lines: PP lens without corrugations. b) Directivity over frequency for PP lenses with and without corrugations, and with an ideal homogeneous matching layer (ML) with constant height.

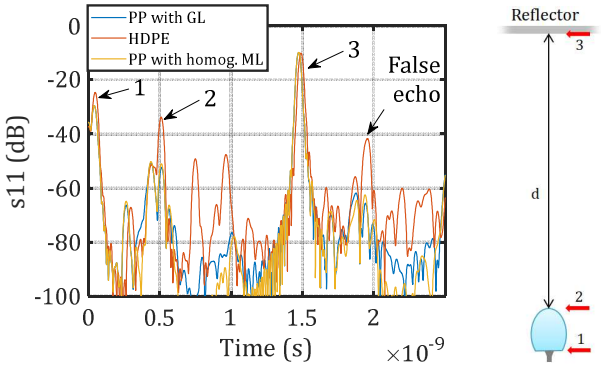

Fig. 8. Time domain reflection coefficient of antenna with metal plate at 100 mm distance. Hanning window applied to results in frequency domain. The arrows point to the reflections in the lens feed, lens-air interface, and target, as indicated in the figure on the right. The false echo generated by the lens multiple reflections is also visible.

CONCLUSION

In this contribution, a low-cost easy to produce lens solution with dielectric gratings is proposed at D-band (110-170 GHz) to reduce false echoes in radar measurements with lens antennas. Standard FFF 3D-printing is used to fabricate the lens in Polypropylene material. The validation of the fabrication accuracy has been carried out at W-band, showing promising results. A prototype at D-band has been fabricated and characterized mechanically, reaching sufficient precision. S-parameter and far-field measurements of the antenna prototype at D-band are scheduled and will be presented in the conference.

ACKNOWLEDGMENT

This work was partially performed within the BANG project, funded by the Federal Ministry for Economic Affairs and Energy under grant number 20Y1901C.

REFERENCES

[1] A. Filippi, V. Martinez, M. Vlot, “Spectrum for Automotive Radar in the 140GHz Band in Europe,” *in Proceedings of EuRAD Conference 2022*, Milano, Italy, 2022.

[2] T. Kürner et al., “Applications Requirement Document (ARD)”, DCN: 15-14-0304-16-003d, IEEE 802.15 TG3d, May 2015, https://mentor.ieee.org/802.15/documents.

[3] E. Tolin *et al.*, "UWB Millimeter-wave 1D MIMO Array for Non-destructive Testing," *2021 15th European Conference on Antennas and Propagation (EuCAP)*, 2021, pp. 1-5

[4] J. Jebramcik, I. Rolfes, N. Pohl and J. Barowski, "Millimeterwave Radar Systems for In-Line Thickness Monitoring in Pipe Extrusion Production Lines," in *IEEE Sensors Letters*, vol. 4, no. 5, pp. 1-4, May 2020.

[5] N. Pohl and M. Gerding, "A dielectric lens-based antenna concept for high-precision industrial radar measurements at 24GHz," *2012 42nd European Microwave Conference*, 2012, pp. 731-734.

[6] A. Neto, S. Maci, P.J.I. de Maagt, “Reflections inside an elliptical dielectric lens antenna,” *IEE Proceedings - Microwaves, Antennas and Propagation*, 1998, 145, (3), p. 243-247.

[7] Andrew J. Gatesman, et al., “An anti-reflection coating for silicon optics at terahertz frequencies,” *IEEE Microwave and Guided Wave Letters*, vol 10, p. 264-266, 2000.

[8] S. Sahin, N. K. Nahar, and K. Sertel, “Thin-film SUEX as an antireflection coating for mmW and THz applications,” *IEEE Trans. THz Sci. Technol.*, vol. 9, no. 4, pp. 417–421, Jul. 2019.

[9] J. Bueno, S. Bosma, T. Bußkamp-Alda, M. Alonso-delPino and N. Llombart, "Lossless Matching Layer for Silicon Lens Arrays At 500 GHz Using Laser Ablated Structures," in *IEEE Transactions on Terahertz Science and Technology*, 2022.

[10] H. Yi, S. -W. Qu, K. -B. Ng, C. H. Chan and X. Bai, "3-D Printed Millimeter-Wave and Terahertz Lenses with Fixed and Frequency Scanned Beam," in *IEEE Transactions on Antennas and Propagation*, vol. 64, no. 2, pp. 442-449, Feb. 2016.

[11] N. T. Nguyen, N. Delhote, M. Ettorre, D. Baillargeat, L. Le Coq and R. Sauleau, "Design and Characterization of 60-GHz Integrated Lens Antennas Fabricated Through Ceramic Stereolithography," in *IEEE Transactions on Antennas and Propagation*, vol. 58, no. 8, pp. 2757-2762, Aug. 2010.

[12] R. J. Friel, M. Gerling-Gerdin, E. Nilsson, and B. P. Andreasson, “3D Printed Radar Lenses with Anti-Reflective Structures,” *Designs*, vol. 3, no. 2, p. 28, Jun. 2019.

[13] B. Derat, S. Schmitz, S. Lachner, M. A. Campo and S. Bruni, "Numerical Modeling and Experimental Validation of a D-band Lens-Based Antenna Design for Beyond 5G Communications," *2020 Antenna Measurement Techniques Association Symposium (AMTA)*, 2020, pp. 1-5.

[14] P. Lalanne, “Effective medium theory applied to photonic crystals composed of cubic or square cylinders,” *Appl. Opt.*, vol. 35, no. 27, p. 5369, Sep. 1996.

[15] M. Arias Campo, D. Blanco, S. Bruni, A. Neto and N. Llombart, "On the Use of Fly’s Eye Lenses with Leaky-Wave Feeds for Wideband Communications," *IEEE Transactions on Antennas and Propagation*, vol. 68, no. 4, pp. 2480–2493, Apr. 2020.

[16] N. Llombart, G. Chattopadhyay, A. Skalare, and I. Mehdi, “Novel terahertz antenna based on a silicon lens fed by a leaky wave enhanced waveguide,” *IEEE Trans. Antennas Propag.*, vol. 59, no. 6, pp. 2160-2168, Jun. 2011.

[17] EMPIRE XPU, Available “http://www.empire.de”.